Rock Mech. Rock Engng. (2004) 37 (4), 331–341
DOI 10.1007/s00603-003-0020-1

Rock Mechanics and Rock Engineering
Printed in Austria

Technical Note

The Influence of Porosity on Tensile and Compressive Strength of Porous Chalks

By

V. Palchik and **Y. H. Hatzor**

Department of Geological and Environmental Sciences, Ben–Gurion University of the Negev, Beer-Sheva, Israel

Received April 3, 2003; accepted September 19, 2003
Published online February 18, 2004

Keywords: Point load strength, Brazilian strength, uniaxial compressive strength, porosity, chalks.

1. Introduction

The compressive and tensile strength of rocks are important design parameters in rock engineering. The uniaxial compressive strength may be obtained via correlation with the point load strength index (D'Andrea et al., 1965; Broch and Franklin, 1972; Pells, 1975; Hassani et al., 1980; Haramy et al., 1981; Kahraman, 2001). In very porous rocks however, porosity has been shown to control the mechanical behavior (e.g. Dunn et al., 1973; Hoshino, 1974; Dearman et al., 1978; Hatzor and Palchik, 1998; Palchik, 1999; Al-Harthi et al., 1999; Palchik and Hatzor, 2002). Porous chalks are quite heterogeneous (Bowden et al., 1998; Bell et al., 1999; Risnes, 2001) and therefore the ultimate strength and deformability typically change within the same formation.

The objective of this paper is to determine the uniaxial compressive strength, point load strength, and indirect tensile (Brazilian) strength of a very porous chalk formation – the Adulam Formation in Israel ($n = 18$–44%), and to study how porosity influences the magnitude of and relationship between these mechanical properties. The obtained results are compared with ISRM suggested methods (ISRM, 1985) for determining point load strength.

2. Experimental Procedures and Results

Specimens for uniaxial compression were surface ground to a roughness smaller than 0.01 mm; specimen ends for point load, Brazilian tests and porosity measurements were

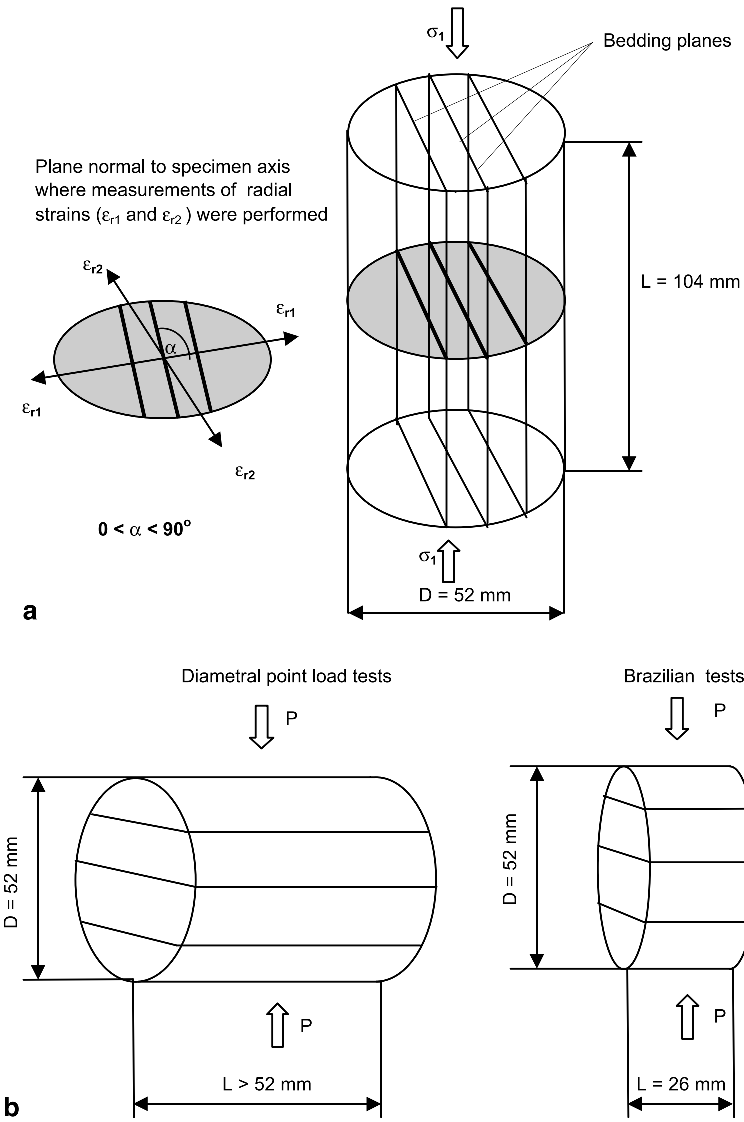

Fig. 1. The relationship between specimen axis, bedding plane direction, and loading direction: **a** uniaxial compression test; **b** point load test and indirect tension (Brazilian) test

ground to a roughness of up to 0.25 mm. Cylinder perpendicularity of all studied specimens was within 0.05 radians. All specimens were cored such that their axis was parallel to bedding (see Fig. 1). All specimens were oven dried at a temperature of 110 °C for 24 h.

2.1 Uniaxial Compressive Strength

Twelve compression tests were performed on 52 mm diameter cylindrical specimens with length/diameter ratio of approximately 2.0 (Fig. 1a). A stiff load frame

Table 1. Results of uniaxial compression tests and porosity calculations for 12 specimens of 52 mm diameter

Sample	E, MPa	ν	σ_c, MPa	ρ_d, g/cm^3	n, %
RC1	17400	0.23	53.2	2.12	21.5
RC2	9300	0.2	20.9	1.85	31.5
RC3	16000	0.26	51	2.07	23.3
RC4	11700	0.2	31.9	1.93	28.5
RC6	19250	0.26	63.3	2.14	20.7
RC7	9500	0.21	32.9	1.89	30
RC8	17300	0.2	60.3	2.11	21.9
RC9	20500	0.27	63.1	2.17	19.6
ST1A	16200	0.31	50.9	2.15	20.5
ST1B	15400	0.23	53.7	2.16	20.2
ST2A	14300	0.2	52.25	2.14	20.7
ST2B	10700	0.22	37.4	2.06	23.7

E elastic modulus, ν Poisson's ratio, σ_c uniaxial compressive strength, ρ_d dry bulk density, n calculated porosity (at $G_s = 2.7$).

332(Terra-Tek, model FX-S-33090) was used which utilizes a closed-loop, servo-controlled hydraulic system with maximum axial force of 1.4 MN and stiffness of $5 * 10^9$ N/m (for load frame details refer to Hatzor and Palchik, 1997). Results of the uniaxial compression tests are presented in Table 1.

Two radial strains were measured in orthogonal directions in a plane normal to the specimen axis (see Figs. 1a and 3a). A comparison between the outputs of radial strain ε_{r1} and radial strain ε_{r2} for all 12 specimens tested under uniaxial compression is plotted

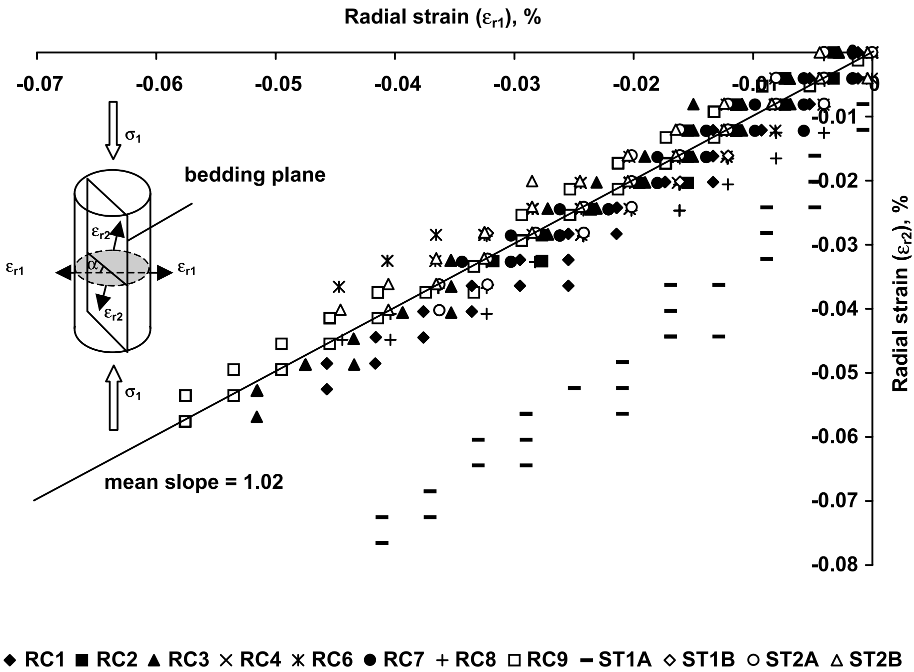

Fig. 2. Comparison between radial strains ε_{r1} and ε_{r2} for 12 specimens tested under uniaxial compression

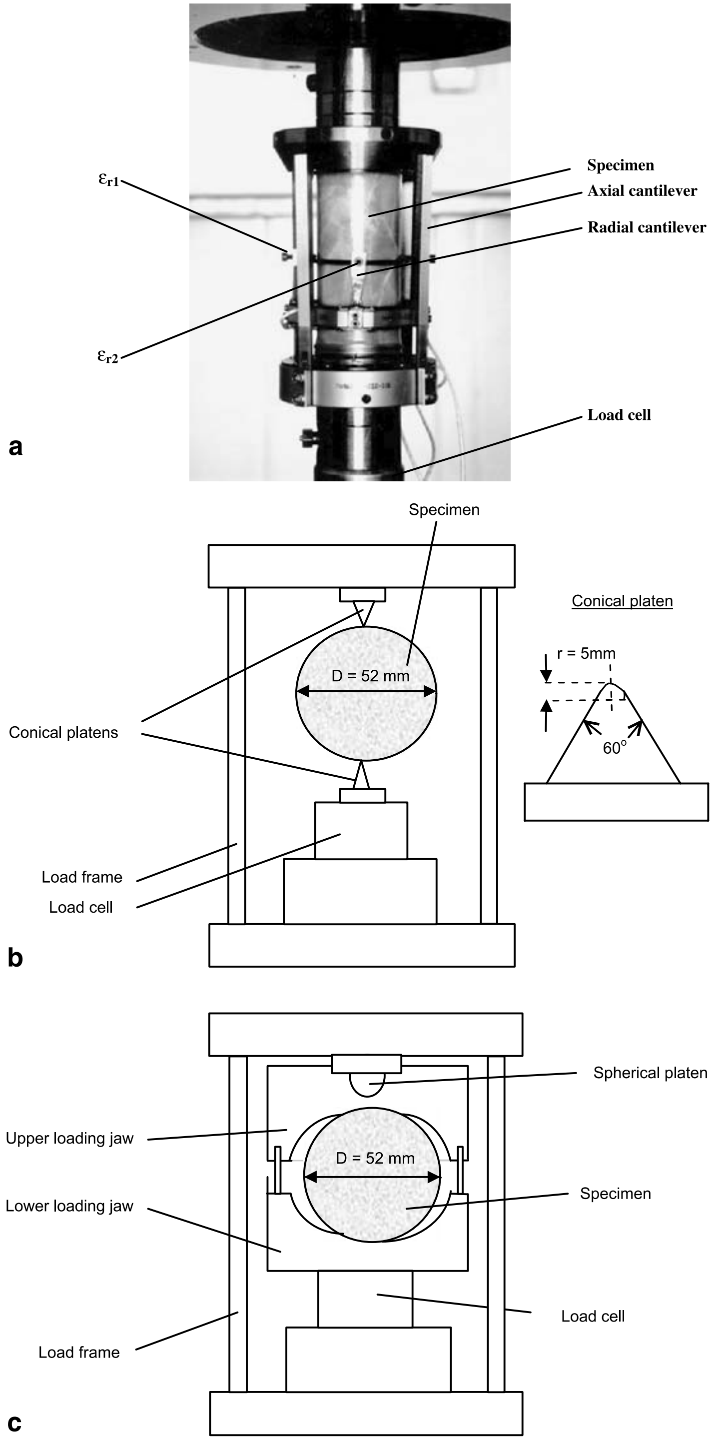

Fig. 3. Test assemblies: **a** for uniaxial compression test; **b** for point load test; **c** for indirect tension (Brazilian) test

in Fig. 2. The obtained linear regressions between ε_{r1} and ε_{r2} are good ($R^2 =$ 0.95–0.99). The symbols reflect radial strain measurements obtained from 0 load to the elastic limit of the stress-strain curve. Consider angle α, defined here as the angle measured on a plane normal to specimen axis, between the bedding plane trace and the axis of ε_{r1} (see Figs. 1a and 2). In our tests the angle α ranged from 0 to 90° – namely, we did not attempt to align the ε_{r1} axis with the bedding plane direction. Nevertheless, the output of the two radial strain transducers was nearly identical in all but one (outlier) case (sample ST1A). Specimen ST1A had initial cracks or veins which probably distorted the radial strain distribution under the applied load. The calculated value of the mean slope is 1.02 with a small standard deviation of 0.1, hence we can establish that the radial strains measured in orthogonal directions are identical. This result suggests transverse isotropy in a plane normal to bedding (or to specimen axis).

2.2 Point Load Strength

Eighteen cylindrical specimens of 52 mm diameter were prepared for diametral point load tests with length/diameter ratio greater than 1.0 (Fig. 1b). Point load testing was performed using a standard Point load/uniaxial Tester (SBEL model PLT-75). A schematic diagram of the point load test assembly is presented in Fig. 3b. The test results are presented in Table 2.

2.3 Indirect Tensile (Brazilian) Strength

Twenty cylindrical specimens of diameter 52 mm were prepared for Brazilian tests. The thickness of the specimen was approximately equal to the specimen radius (Fig. 1b). Indirect tensile (Brazilian) strength was obtained using the same Point load/uniaxial

Table 2. Results of point load tests and porosity calculations for 18 specimens of 52 mm diameter

Sample	ρ_d, g/cm^3	n, %	I_d, MPa
PL1	1.89	29.9	2.86
PL2	2.1	22.2	3.54
PL3	2.18	19.1	4.28
PL4	2.09	22.6	3.25
PL5	1.93	28.7	2.58
PL6	1.76	35	1.85
PLA1	1.84	32	2.31
PLA2	1.78	34.2	1.72
PLA3	1.76	35	1.83
PLB1	1.65	39	1.69
PLB2	1.7	37	1.78
P1	2.09	22.5	3.11
P2	1.67	38.3	2.27
P3	2.06	23.6	2.82
P4	2.05	23.9	2.97
P5	2.19	18.9	3.37
P6	1.93	28.6	2.98
P7	1.73	36	1.84

ρ_d dry bulk density, n calculated porosity (at $G_s = 2.7$), I_d point strength.

Table 3. Results of Brazilian tests and porosity calculations for 20 specimens of 52 mm diameter

Sample	ρ_d, g/cm^3	n, %	σ_t, MPa
BT1	2	26.1	7.49
BT2	2.06	23.6	8.58
BT3	2.04	24.4	5.49
BT4	1.86	31	4.47
BT5	1.93	28.4	3.59
BT6	1.87	30.7	4.36
BLA1	1.65	38.9	5.17
BLA2	1.52	43.9	2.85
BLA3	1.92	28.7	6.9
BLB1	2.02	25.3	8.01
BLB2	2.13	21.2	8.74
BLB3	1.86	31.1	6.35
B1	1.68	37.6	3.9
B2	1.76	35	4.4
B3	1.53	43.4	2.5
B4	2.03	24.7	5.6
B5	1.91	29.4	5.04
B6	1.7	37.2	4.96
B7	1.69	37.6	2.92
B8	2.06	23.8	6.48

ρ_d dry bulk density, n calculated porosity (at $G_s = 2.7$), σ_t tensile (Brazilian) strength.

SBEL Tester (model PLT-75). Here however, loading was applied by two diametrically-opposed concave loading jaws (Fig. 3c). Since the isotropy of the studied chalk in a plane normal to bedding was confirmed in the uniaxial tests discussed above, there was no need to align the conical platens or loading jaws with the trace of bedding planes in point load or Brazilian tests, respectively. Indirect tensile strength results (σ_t) are presented in Table 3.

3. Porosity

3.1 Porosity Calculation

The porosity of 50 dry specimens from Tables 1–3 was calculated prior to mechanical testing. The porosity (n) of the solid-cylinder chalk specimens was obtained by the expression $n = [1 - \rho_d/(G_s\rho_w)] * 100\%$ using measured values of dry bulk density (ρ_d, g/cm^3), water density $\rho_w = 1\text{g/cm}^3$, and assumed specific gravity of $G_s = 2.7$ which is typical for calcite. The G_s assumption was validated using porosimeter measurements (Section 3.2 below). The calculated porosity values ranged between 18% and 44%. The precision of the calculated values is to be within 0.1%. Bulk density and porosity values for all 50 specimens are presented in Tables 1–3.

3.2 Porosity Measurement

A Helium porosimeter (CoreTest Inc., model PHI-220) was used to confirm the validity of the porosity estimations. In order to determine the porosity of the studied

Table 4. Bulk volume, dry bulk density, grain volume observed in Helium porosimeter PHI-220, and calculated porosity of 10 specimens (diameter of 25.4 and 38 mm)

Sample	V_{bulk}, cm^3	ρ_d, g/cm^3	V_{grain}, cm^3	$n_{porosim}$, %	n, %
$PS1_{(25.4)}$	11.43	2.13	9.09	20.4	21.2
$PS2_{(25.4)}$	10.87	2.13	8.68	20.1	21.1
$PS3_{(25.4)}$	11.55	2.13	9.13	21	21.2
$PS4_{(25.4)}$	11.61	1.72	7.65	34.1	36.1
$PS5_{(25.4)}$	11.78	1.9	8.37	29	29.8
$PS6_{(25.4)}$	11.95	2	8.93	25.3	26
$PS7_{(25.4)}$	12	1.83	8.17	31.9	32.4
$PS8_{(25.4)}$	11.82	1.96	8.64	27	27.3
$PM1_{(38)}$	40.9	2.28	34.9	14.7	15.6
$PM3_{(38)}$	41	2.26	34.3	16.3	16.3

(25.4) and (38) specimen diameter in mm, V_{bulk} bulk volume, ρ_d bulk dry density, V_{grain} grain volume, $n_{porosim}$ porosity observed using Helium porosimeter, n calculated porosity (at $G_s = 2.7$).

chalks, eight specimens of diameter 25.4 mm and two specimens of diameter 38 mm with length of 25.4 and 38 mm, respectively, were examined. The determination of pore volume was not performed by direct measurement because direct pore volume measurement requires previous determination of the so-called "dead volume" in the porosimeter. Measurement of "dead volume" requires an additional apparatus (a coreholder) which was not used in this research. Therefore, we used the porosimeter to determine the grain volume, and then calculated the pore volume using the measured bulk volume (with 10 micrometer resolution calipers) and the measured grain volume (using the porosimeter). The obtained porosity is referred to as 'measured' porosity below.

Results of bulk volume (V_{bulk}), dry bulk density (ρ_d), grain volume (V_{grain}), 'measured' porosity ($n_{porosim}$), and calculated porosity (n, with $G_s = 2.7$), for all specimens tested in the Helium porosimeter are presented in Table 4. Since a very good linear correlation ($R^2 = 0.99$) is found between the calculated and 'measured' porosity values, we conclude that the assumption of $G_s = 2.7$ is justified for the studied chalks.

4. Discussion

4.1 Point Load and Brazilian Strength

The effect of porosity on point load strength (I_d) and Brazilian tensile strength (σ_t) is presented in Fig. 4a from which three trends may be inferred:

1. Both point load and Brazilian strength indices are inversely related to porosity.
2. The correlation between porosity and point load strength is good: point load strength rapidly decreases with increasing porosity. The relationship follows an exponential law with a reasonable squared regression coefficient ($R^2 = 0.84$) which can be described by:

$$I_d = ce^{-dn} \tag{1}$$

where c and d are empirical coefficients which for Adulam chalks are: $c = 7.74$, $d = 0.039$.

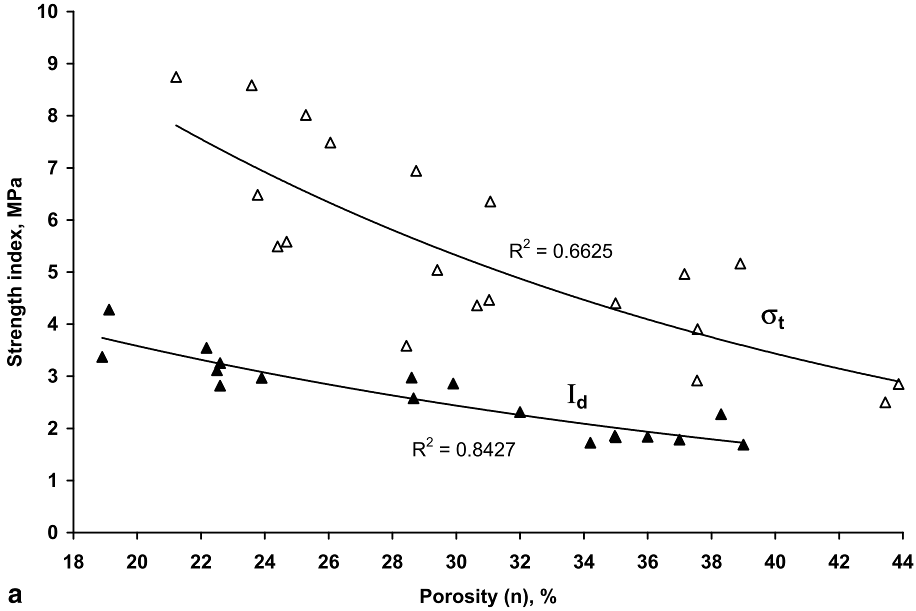

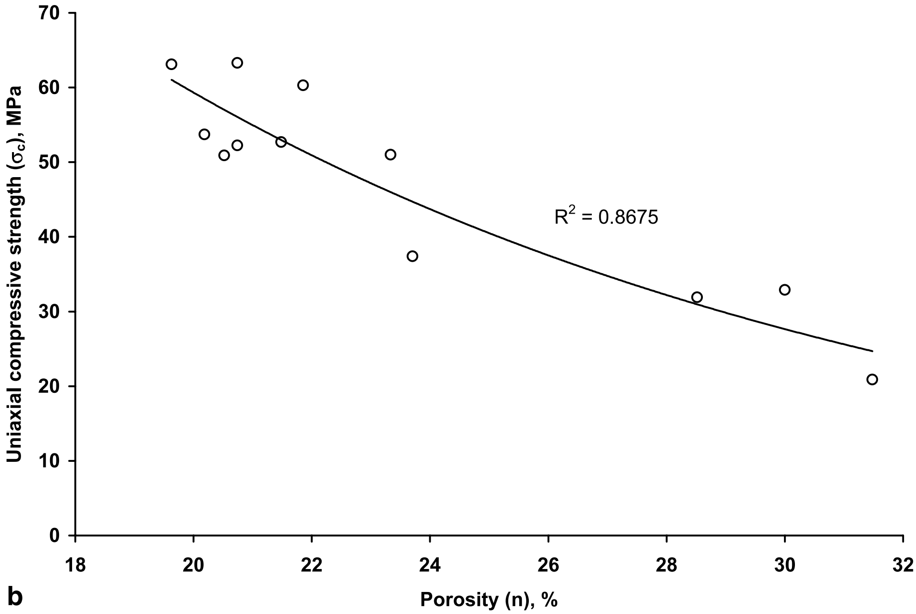

Fig. 4. Influence of porosity on mechanical strength: **a** point load strength (I_d) and Brazilian strength (σ_t); **b** uniaxial compressive strength (σ_c)

3. The correlation between Brazilian strength (σ_t) and porosity is somewhat weaker ($R^2 = 0.66$). Therefore, a mathematical model for this dependence is not suggested here, although a trend clearly exists. Similarly, an explicit model for $I_d/\sigma_t = f(n)$ is not suggested here.

4.2 Uniaxial Compression

The relationship between uniaxial compressive strength and porosity is shown in Fig. 4b, which displays results from all 12 uniaxial compression tests. A good correlation is obtained which follows an exponential law ($R^2 = 0.87$):

$$\sigma_c = ae^{-bn} \tag{2}$$

where a and b are empirical coefficients which for Adulam chalks are: $a = 273.15$, $b = 0.076$.

4.3 The Ratio Between Uniaxial and Point Load Strength (σ_c/I_d)

The point load test may be used as an index property in rock engineering applications where in fact the true uniaxial compressive strength is sought. This is because obtaining point load strength data is by far simpler than obtaining actual uniaxial compression test data, which requires strict adherence to sample preparation standards and sophisticated testing techniques. Therefore, it has become standard practice to rely on published correlations for predicting uniaxial strength from point load data. For 50 mm diameter core samples the typical correlation is: $\sigma_c/I_d = 20–25$ (ISRM, 1985).

In this section we explore the role of porosity and how it influences the correlation between point load and uniaxial compressive strength. In Eq. (1) the influence of porosity on point load index was given and in Eq. (2) the influence of porosity on

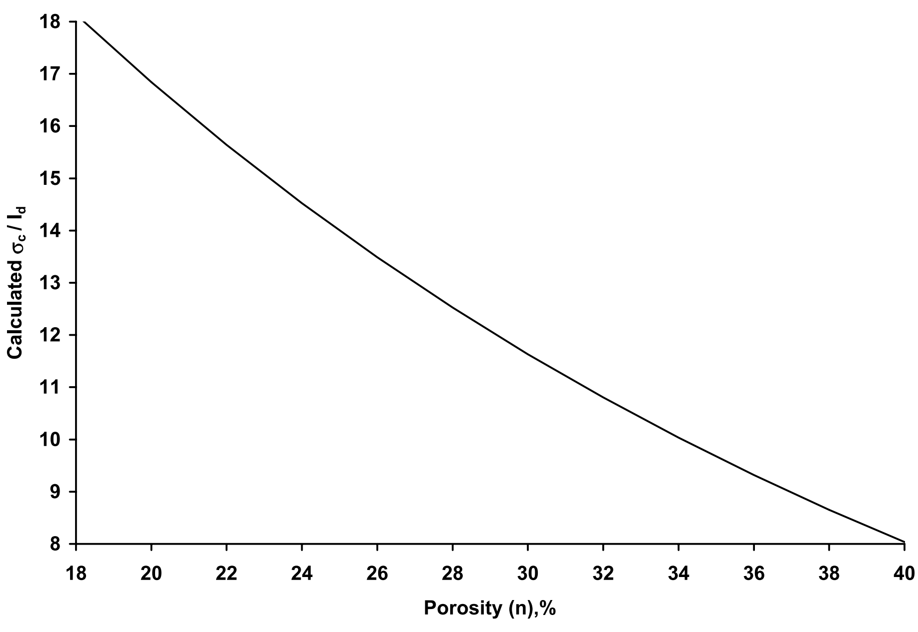

Fig. 5. Calculated effect of porosity on the ratio between uniaxial compressive strength and point load strength, for studied chalks

true uniaxial compressive strength was described. Using Eq. (1) and Eq. (2) we can write a new expression for the ratio between uniaxial compressive and point load strength, as a function of porosity:

$$\frac{\sigma_c}{I_d} = k_1 e^{-k_2 n} \tag{3}$$

where k_1 and k_2 are empirical coefficients which can be calculated from coefficients *a*, *b*, *c* and *d*: $k_1 = a/c = 35.3$, $k_2 = b - d = 0.037$.

The empirical relationship suggested in Eq. (3) is plotted in Fig. 5, where it is shown that the ratio σ_c/I_d decreases exponentially from 18 to 8 with increasing porosity (*n*) values from 18% to 40%. Hence, an increase in porosity by a factor of 2.2 leads to decrease in the ratio σ_c/I_d by a factor of 2.25.

We can conclude therefore that the ratio between uniaxial compressive strength and point load strength within the same heterogeneous chalk formation may not be constant, but is porosity dependent. Furthermore, it may be inferred from Fig. 5 that weaker (higher porosity) chalks have a lower σ_c/I_d ratio, whereas stronger chalks (lower porosity) have a higher σ_c/I_d ratio.

5. Conclusions

Point load strength, indirect (Brazilian) tensile strength, uniaxial compressive strength and porosity of Adulam chalk in Israel were studied using dry cylindrical specimens with the same orientation (specimen axis parallel to bedding). The validity of the porosity calculation was confirmed by measuring grain volume using a Helium porosimeter.

It was established that the point load strength and uniaxial compressive strength in porous Adulam chalks decrease with increasing porosity, while the same effect of porosity on Brazilian tensile strength was present but not significant. Two exponential models relating porosity to uniaxial and point load strengths are proposed.

Our observations also show that the ratio σ_c/I_d between uniaxial compressive strength and point load strength is not constant (range 8–18), but is porosity dependent. An increase in porosity from 18 to 40% leads to decrease in σ_c/I_d from 18 to 8. The difference between the observed ratio (8–18) and standard practice ($\sigma_c/I_d = 20$–25), according ISRM suggested method (ISRM, 1985) can be as high as 127%.

References

Al-Harthi, A. A., Al-Amri, R. M., Shehata, W. M. (1999): The porosity and engineering properties of vesicular basalt in Saudi Arabia. Engng. Geol. 54, 313–320.

Bell, F. G., Culshaw, M. G., Cripps, J. C. (1999): A review of selected engineering geological characteristics of English chalk. Engng. Geol. 54(3–4), 237–269.

Bowden, A. J., Lamont-Black, J., Ullyott, S. (1998): Point load testing of weak rocks with particular reference to chalk. Quarterly J. Engng. Geol. 31(2), 95–103.

Broch, E., Franklin, J. A. (1972): The point-load strength test. Int. J. Rock Mech. Sci. 9, 669–697.

D'Andrea, D. V., Fischer, R. L., Fogelson, D. E. (1965): Prediction of compressive strength from other rock properties. Rep. Invest. US. Bur. Mines. 6702, 23 pp.

Dearman, W. R., Baynes, E. J., Irfan, T. Y. (1978): Engineering grading of weathered granite. Engng. Geol. 12, 345–374.

Dunn, D. E., LaFountain, L. J., Jackson, R. E. (1973): Porosity dependence and mechanism of brittle fracture in sandstones. J. Geophys. Res. 78, 2403–2417.

Haramy, K. Y., Morgan, T. A., DeWaele, R. E. (1981): A method for estimating coal strengths from point load tests on irregular lumps. USBM, Denver Reseach Center, Progress Rept., 10028, 31 pp.

Hassani, F. P., Scoble, M. J., Whittaker, B. N. (1980): Application of the point load index test to strength of rock, and proposals for a new size correction chart. Proc. 21st US Symp. on Rock Mechanics, Rolla, Missouri, 543–556.

Hatzor, Y. H., Palchik, V. (1997): The influence of grain size and porosity on crack initiation stress and critical flaw length in dolomites. Int. J. Rock Mech. Min. Sci. 34(5), 805–816.

Hatzor, Y. H., Palchik, V. (1998): A microstructure – based failure criterion for Aminadav dolomites. Int. J. Rock Mech. Min. Sci. 35(6), 797–805.

Hoshino, K. (1974): Effect of porosity on strength of clastic sedimentary rock. Proc. 3rd Cong. Int. Soc. Rock Mech., Denver, CO, A. A. Balkema, Rotterdam, 1, 511–516.

ISRM, International Society of Rock Mechanics (1985): Suggested method for determining point load strength. Int. J. Rock Mech. Min. Sci. 22, 53–60.

Kahraman, S. (2001): Evaluation of simple methods for assessing the uniaxial compressive strength of rock. Int. J. Rock Mech. Min. Sci. 38, 981–994.

Palchik, V. (1999): Influence of porosity and elastic modulus on uniaxial compressive strength in soft brittle porous sandstones. Rock Mech. Rock Eng. 32(4), 303–309.

Palchik, V., Hatzor, Y. H. (2002): Crack damage stress as a composite function of porosity and elastic matrix stiffness in dolomites and limestones. Engng. Geol. 63(3–4), 233–245.

Pells, P. J. N. (1975): The use of the point load test in predicting the compressive strength of rock materials. Aust. Geomech. J. G5, 54–56.

Risnes, R. (2001): Deformation and yield in high porosity outcrop chalk. Physics and chemistry of the Earth, Part A: Solid Earth and Geodesy 26(1–2), 53–57.

Author's address: Dr. V. Palchik, Department of Geological and Environmental Sciences, Ben–Gurion University of the Negev, P.O. Box 653, Beer-Sheva, 84105, Israel; e-mail: vplachek@bgumail.bgu.ac.il